RSC Advances

PAPER

View Article Online
View Journal | View Issue

Cite this: *RSC Adv.*, 2021, **11**, 35287

Optimized energetic HNTO/AN co-crystal and its thermal decomposition kinetics in the presence of energetic coordination nanomaterials based on functionalized graphene oxide and cobalt†

Sabrina Hanafi,[a] Djalal Trache,*[a] Abderrahmane Mezroua,[a] Hani Boukeciat,[a] Redha Meziani,[a] Ahmed Fouzi Tarchoun[ab] and Amir Abdelaziz[a]

The present research aims to select the optimal molar ratio of hydrazine 3-nitro-1,2,4-triazol-5-one (HNTO) and ammonium nitrate (AN) to produce an energetic co-crystal. For a comparison purpose, the heat release, cost, density and hygroscopicity of the different co-crystals were evaluated. The obtained results indicated that HNTO/AN at the 1 : 3 ratio exhibited a higher heat release, better thermal stability, low water content and a reasonable cost, compared to other co-crystals. This new co-crystal was fully characterized through powder X-ray diffraction (XRD), infrared spectroscopy (FTIR) and differential scanning calorimetry (DSC), confirming that this latter displayed similar characteristics to those of the co-crystal with a 1 : 1 ratio, which was recently developed. On the other hand, the catalytic activity of two energetic coordination polymers of triaminoguanidine-cobalt (T-Co) complexes, with or without graphene oxide (GO-T-Co-T), on the thermolysis of the developed co-crystal has been also assessed by DSC under non-isothermal conditions. It is revealed that these catalysts have greatly decreased the decomposition temperature of the HNTO/AN cocrystal. Moreover, because of the complete decomposition in the case of the (HNTO/AN)/GO-T-Co-T composite, the heat release has been increased as well. Isoconversional integral kinetic methods were exploited to determine the kinetic parameters of the different systems. According to the obtained results, these catalysts have a strong catalytic action on the decomposition of the co-crystal AN/HNTO for which the activation energy and the pre-exponential factor are considerably lowered. Consequently, the developed co-crystal and the energetic catalysts could be considered as potential ingredients for the next generation of composite solid propellant formulations.

Received 23rd August 2021
Accepted 21st October 2021

DOI: 10.1039/d1ra06367g

rsc.li/rsc-advances

1. Introduction

The development of new energetic materials (EMs), which display a very low sensitivity, good stability and better performance, has attracted a tremendous amount of attention from the scientific community worldwide.[1] These EMs, encompassing propellants, explosives and pyrotechnics, play a prominent role in several applications to meet the growing needs of the modern society.[2,3] They usually release a huge amount of energy/force in a short time upon ignition or initiation to ensure a specific function for a wide range of civilian and military uses.[4]

The key performance metrics for EMs comprise the thermal stability, sensitivity, density, oxygen balance, shape/size factors, and combustion/detonation parameters.[5,6] Nowadays, numerous in-depth research works have been performed to overcome the challenge of the production of novel insensitive high performance EMs such as, nitro-compounds,[7] poly-nitrogen compounds,[8] energetic ionic liquids,[9] energetic salts,[10] and energetic super-molecules like host/guest complexes and co-crystals,[11,12] to cite a few. However, experts in the field have revealed that it is commonly problematic to balance between satisfactory stability, sensitivity and performance for suitable storage, handling, transportation, and uses of advanced EMs.[13] Consequently, it is prerequisite to address such drawbacks through the employment of modern approaches such as coating technologies, doping with inert/energetic ingredients, and co-crystallization processes, which proved their efficiency during the last few years, to synthesis and design novel EMs with tailorable properties.[14]

[a]*Energetic Materials Laboratory, Teaching and Research Unit of Energetic Processes, Ecole Militaire Polytechnique, BP 17, Bordj El-Bahri, Algiers, 16046, Algeria. E-mail: djalaltrache@gmail.com*

[b]*Energetic Propulsion Laboratory, Teaching and Research Unit of Energetic Processes, Ecole Militaire Polytechnique, BP 17, Bordj El-Bahri, Algiers, 16046, Algeria*

† Electronic supplementary information (ESI) available. See DOI: 10.1039/d1ra06367g

It is worthy to mention that the development of new effective pure EMs is not so simple, since it is confronted with different problems such as the complexity and the time-consuming of the processes, requiring several reaction steps, as well as the challenge of process scaling-up. Therefore, the modification of the existing high EMs such as ammonium nitrate (AN), octahydro-1,3,5,7-tetranitro1,3,5,7-tetrazocine (HMX), 2,4,6,8,10,12-hexanitro-2,4,6,8,10,12-hexazisowurtzitane (CL-20), 3-nitro-1,2,4-triazol-5-one (NTO), among others, rather than developing new ones, through the optimization of the above-mentioned approaches will certainly improve their physicochemical features and performance to extend their applicability.[15]

Co-crystallization has been shown as one of the most promising routes to achieve energetic materials with appropriate physicochemical and energetic properties.[16] It may modify the crystal structure and the internal composition of EMs without affecting the molecular structure of the pristine EMs. Thus, a co-crystal is a new crystal constituted by two or more chemical elements with a proper stoichiometric ratio linked with hydrogen bonding, van der Waals forces, p–π stacking and π–π stacking, and/or other non-covalent interactions.[17–19] Several energetic co-crystals with interesting features have been developed so far and the topic continues to attract current/future and increasingly intense international discussion to fulfill the requirement of the next generation of EMs.[20–22]

As one of the most interesting propellant oxidizer and explosive ingredient, AN displays prominent characteristics such a positive oxygen balance, low cost, availability, and 100% of gaseous decomposition products.[23] Nonetheless, AN exhibits unneglectable shortcomings such as low energy rate, poor ignitability, lower burning rate, high hygroscopicity, and an ambient temperature polymorphic solid–solid phase transition, acknowledged as one of the foremost reason for damaging and caking of AN-based energetic formulations, which inhibits its extensive employments, particularly as solid-propellant ingredient.[24] Within this framework, numerous research activities have been performed to surpass its above-stated issues and promote its utilization as a green oxidizer. Trache *et al.* have claimed that the co-crystallization of AN with other energetic co-formers is a potent methodology to overcome its lower performance and decreased reactivity.[25] For example, Lee *et al.* prepared a c-crystal of AN and crow ethers,[26] demonstrating that this latter showed good flowability, smokeless and non-hygroscopicity. In another work, Kumar *et al.* produced AN-based co-crystal with potassium dinitramide (KDN) at a 1 : 1 mass ratio.[27] It was proved that KDN efficiently stabilized AN and improved its burning features. Recently, AN/saccharides co-crystal was prepared by Oluwoye *et al.*, revealing that this latter that exhibits promising burning characteristics and low hygroscopicity can undoubtedly used as solid propellant oxidizer.[28] More recently, our research group developed a co-crystal of AN with hydrazine 3-nitro-1,2,4-triazol-5-one (HNTO) with a molar ratio of 1 : 1.[29] It was proved that the obtained energetic–energetic co-crystal allowed achieving desirable features such as the elimination of the solid–solid thermal transitions, higher energy content and density, good thermal stability, and improved sensitivity. However, the employment of a higher amount of HNTO (50%) at large-scale can inhibits the use of this co-crystal as propellant oxidizer because of the high production cost of HNTO compared to that of AN on one hand, and its negative oxygen balance (−38%), which decreases the overall oxygen balance of the co-crystal on the other hand. Thus, assessing the feasibility of producing AN/HNTO co-crystal with a higher amount of AN with respect to that of HNTO, while maintaining the same performance or even better that of the co-crystal prepared at ratio of 1 : 1 is more than necessary.

On the other hand, to fully exploit EMs and ensure their energy release more efficiently, several compounds at different shape and size, known as combustion catalysts, maybe incorporated at a small amount.[30–33] Two-dimensional complex structures based on graphene oxide (GO) were reputed to be as effective energetic catalysts for several energetic materials.[34] Nowadays, a number of 2-D layered energetic hybrid crystals have been produced through the bridging of GO layers with triaminoguanidine (T) and subsequently functionalized with extra T-coordinated with transition metal ions from their respective perchlorate and nitrates. Recently, our research group designed GO-doped transition metal (Co) complexes of T and assessed their catalytic effect toward ammonium perchlorate, RDX, and NTO.[35,36] However, to the best knowledge of the authors, such type of catalysts has never been applied as additive of energetic co-crystals. Besides that, the use of GO as catalytic support may play a synergistic effect with the other ingredients, which will enhance the stability as well the decomposition efficient of the developed energetic co-crystals.[37]

To provide a better insight about the effect of molar ratios of HNTO and AN co-formers on the produced co-crystal and selecting the optimal composition, following the same process reported in our previous work, the present work was carefully implemented. The obtained co-crystals were fully analyzed in terms of density, hygroscopicity, released energy and production cost to select the optimal co-crystal composition. This latter is also compared to the co-crystal of a molar ratio 1 : 1, developed in our recent work,[29] in terms of structure and thermal behavior in a detailed manner. After that, a deep investigation of the catalytic effect of the two high energetic 2D-catalysts, namely, T-Co and GO-T-Co-T, developed in our previous study,[35] on the thermolysis of HNTO/AN by means of non-isothermal differential scanning calorimetry (DSC). The kinetic parameters, including the energy of activation, pre-exponential factor and the reaction models of the co-crystal supplemented with catalysts have been calculated by means of four isoconversional integral methods, *viz.*, Trache–Abdelaziz–Siwani (TAS), iterative Kissinger–Akahira–Sunose (it-KAS), iterative Flynn–Wall–Ozawa (it-FWO) and Sbirrazzuoli methodology.

2. Experimental section

2.1. Samples

Pure HNTO was prepared in our laboratory following the same approach described in the literature,[38,39] whereas AN with a purity of 99.9% was purchased from VWR-Prolabo. The

methodology used to prepare T-Co and GO-T-Co-T complexes was comprehensively elaborated in our recent paper.[35] All the used chemicals were supplied by Sigma-Aldrich, and were used as received without any supplementary purifications.

2.2. Co-crystal preparation at different molar ratios

Knowing that the energetic co-crystal properties like stability, density, mechanical properties, sensitivity performance are likely affected by the molar ratio of the co-formers. Thus, to rationalize the amount of HNTO and well valorize the employment of AN, several amounts of AN and HNTO have been tested. Crystallization experimentations have been conducted by dissolving different molar proportion (1 : 1, 1 : 2, 1 : 3, 1 : 4, 1 : 5, 1 : 6, 1 : 7, 1 : 9) of HNTO and AN, respectively, in anhydrous methanol (20 mL). Each mixture was stirred at a temperature of 45 °C during 30 min, and then dried by the evaporation of the solvent under ordinary conditions to produce different HNTO/AN products. The detailed procedure of the synthesis of the co-crystals is depicted in Fig. 1.

2.3. Preparation of co-crystal@catalyst mixtures

After selecting the best co-crystal, which corresponded to the molar ratio of 1 : 3, 160 mg of it was put into 30 mL of acetone and 40 mg catalyst (T-Co or GO-T-Co-T) for which the preparation pathway characterization were provided in the ESI† were added to the mixture. The solution was stirred to ensure the homogenization of the mixtures, and then dried in air to provide HNTO/AN@T-Co and HNTO/AN@GO-T-Co-T composites, respectively. A schematic presentation of the preparation of the mixtures is also provided in Fig. 1.

3. Characterizations

3.1. Thermal analyses

DSC experiments were recorded using a PerkinElmer DSC8000 instrument. Beforehand, a calibration of the apparatus using high pure indium and zinc was carried out. Samples were placed in aluminum crucibles with pinhole in the lid to avoid pressure build up in the pans during heating. DSC measurements were realized under a nitrogen gas atmosphere (50 mL min^{-1}) within a temperature range of 25–350 °C. The heating rates of 5, 10, 15, 20 °C min^{-1} were used for the kinetic investigation. Pyris software was employed for data acquisition and their processing. The uncertainties associated with the thermal properties were evaluated based on repeated measurements (threefold) and found to be within ±0.1 K for the decomposition temperature and 10 J g^{-1} for the enthalpy.

A thermogravimetric analyzer model Q50, TA Instruments was used to follow the mass change. The different obtained co-crystals have been subjected to a constant temperature of 120 °C for 60 min under nitrogen flow atmosphere with a sample mass

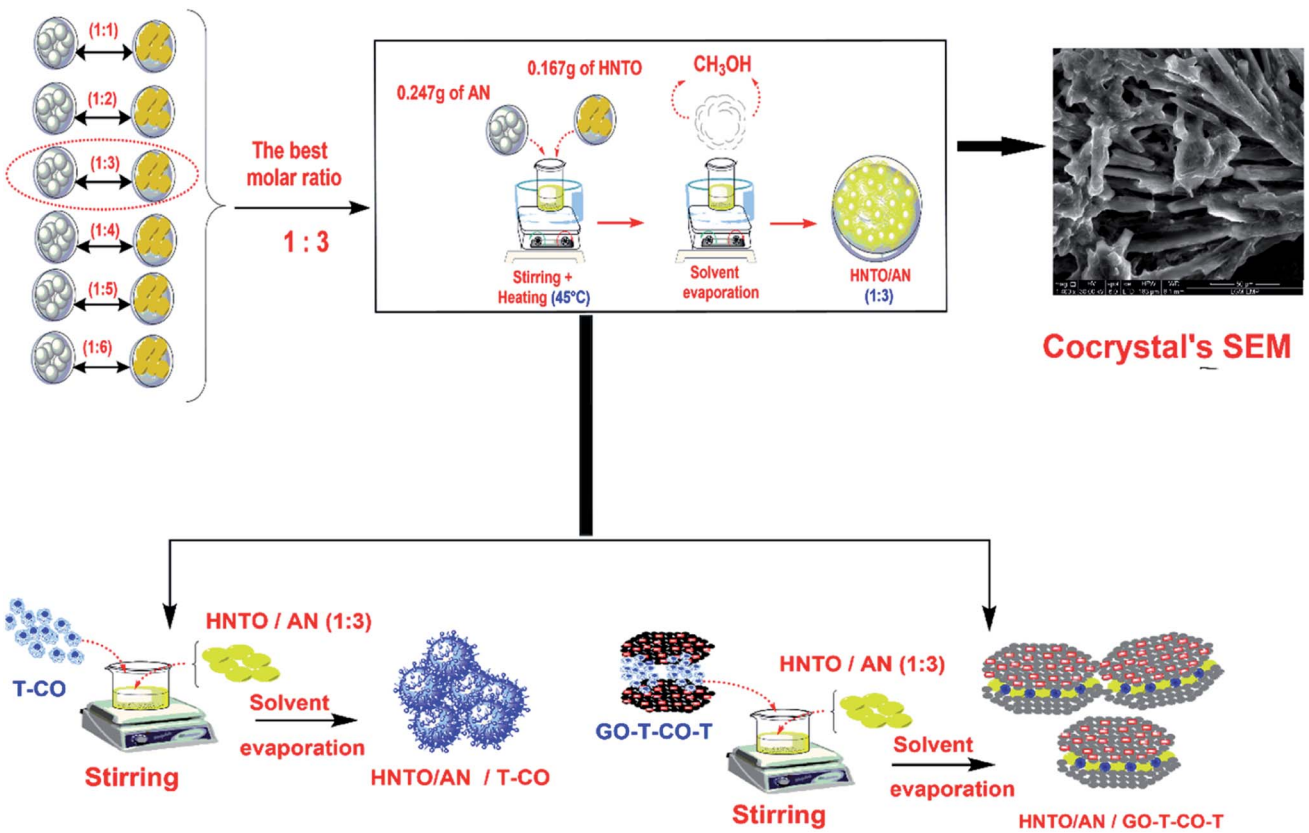

Fig. 1 Preparation procedure of the co-crystal coated with cobalt metal complexes of triaminoguanidine (T-Co) and cobalt metal complexes of triaminoguanidine doped with GO (GO-T-Co-T).

of 5 mg at a heating rate of 10 °C min^{-1}. This analytical technique has been used in order to evaluate the moisture content of the developed co-crystals.

3.2. Density measurement

Sample density is one of the main important physical properties of EMs.[40] It may affect the performance of the products. An electronic densimeter, type Accupyc 1340 II Pycnometer (Micromeritics) has been used to determine the density of the studied samples at a temperature of 25.4 ± 0.5 °C. Ten experiments were performed for each individual system in order to calculate the mean density and the standard deviation.

3.3. FTIR spectroscopy

The FTIR technique was carried out with a PerkinElmer spectrometer. The spectra were recorded in transmittance mode within the wavenumber range of 400–4000 cm^{-1}. Spectra were collected with a wavenumber resolution of 4 cm^{-1}. To accomplish a suitable signal-to noise ratio, different measurements were taken with 64 scans.

3.4. XRD measurement

X-ray diffractometer, a very useful tool to get a deeper understanding about the formation of co-crystal,[41] is employed. A PANalytical X'pert PRO Multi-Purpose diffractometer has been utilized for the collection of the powder XRD patterns at a current and voltage generator of 40 mA and 45 kV, respectively, with Cu-Kα radiation. The spectra were collected by scanning 2θ from 5° to 50°.

3.5. SEM analysis

The morphological characteristics of the investigated samples were performed using an FEI Quanta 600 with a working distance of 10 mm at 10 kV accelerating voltage. The samples were dried and placed on a sticky carbon bad and coated with a conductive carbon films before experiment.

3.6. Kinetic modeling

The kinetic triplet can be calculated by using two methods: isoconversional and non-isoconversional. Integral isoconversional methods are the methods recommended by International Confederation for Thermal Analysis and Calorimetry kinetics committee (ICTAC) because they provide the kinetic parameters without assuming a particular reaction model, and they are not sensitive to experimental noise. Moreover, these methods give results that are more reliable since they use multiple temperature programs.[42]

In this study, kinetic parameters were estimated through four isoconversional methods namely, TAS,[43] it-KAS,[44] VYA[45] and it-FWO.[46]

Generally, the rate of many thermally stimulated methods may be described as follows, in terms of α and T:

$$\frac{d\alpha}{dt} = k(T)f(\alpha) \quad (1)$$

where t, α and T refer respectively to time, the extent of conversion and temperature. $k(T)$ is the rate constant, and $f(\alpha)$ is the mathematical function of the reaction mechanism.

In fact, α value, in this paper, is experimentally derived from DSC thermal analysis technique as a fraction change of as the ratio of the current heat change ΔH to the total heat released or adsorbed ΔH_{tot}: like defined in eqn (2).

$$\alpha = \frac{\int_{t_0}^{t}(dH/dt)dt}{\int_{t_0}^{t_f}(dH/dt)dt} = \frac{\Delta H}{\Delta H_{total}} \quad (2)$$

Conferring to the Arrhenius law, the temperature dependence $k(T)$, can be written as shown in eqn (3)

$$\frac{d\alpha}{dt} = Ae^{-\frac{E_a}{RT}}f(\alpha) \quad (3)$$

where T refers to the reaction temperature and R is the universal gas constant and E_a and A stand for kinetic parameters.

Moreover, the temperature program can be isothermal or non-isothermal. Non-isothermal program which is the most commonly utilized is that in which the temperature changes linearly with time, as illustrated in eqn (4)

$$\beta = \left(\frac{dT}{dt}\right) \quad (4)$$

Elseways, the first term in eqn (3) may be readjusted as below:

$$\frac{d\alpha}{dt} = \left(\frac{d\alpha}{dT}\right)\left(\frac{dT}{dt}\right) = \beta\left(\frac{d\alpha}{dT}\right) \quad (5)$$

The combination of eqn (5) and (3) conduct to:

$$\frac{d\alpha}{dT} = \frac{A}{\beta}e^{-\frac{E_a}{RT}}f(\alpha) \quad (6)$$

The integration of eqn (6) lead to

$$g(\alpha) = \int_0^{\alpha}\frac{d\alpha}{f(\alpha)} = \frac{A}{\beta}e^{-E_a/RT}dT \quad (7)$$

$g(\alpha)$: the integral reaction model. In fact, 41 forms of $g(\alpha)$ are reported in the work of Trache *et al.*[43]

Isoconversional methods or model free methods is one of the most used approaches.[47,48] Herein, four isoconversional integral methods were chosen to study the kinetic of the different systems *Viz.* VYA, it-FWO, it-KAS and TAS.

To star, the conversion dependent activation energy of TAS method is obtained by using the modified Coats–Redfern (MCR), which is given in eqn (8).

$$\ln\left[\frac{\beta_i}{{T_{\alpha,i}}^2(1-2RT_{\alpha,i}/E_{\alpha,i})}\right] = \ln\left[\frac{A_\alpha R}{g(\alpha)E_{\alpha,j+1}}\right] - \frac{E_{\alpha,j+1}}{RT_{\alpha,i}} \quad (8)$$

j refers to the number of iteration and i is the experiments number.

The combination of the intercept of the MCR equation, the 41 kinetic models and the compensation effect (CE) equation at

an iteration n lead to obtain $g(\alpha)$ and the compensation parameters a and b:

$$I_\alpha(n) = \ln\left[\frac{A_\alpha R}{g(\alpha)E_{\alpha,n}}\right] \quad (9)$$

$$I_\alpha(n) - \ln\left[\frac{R}{g(\alpha)E_{\alpha,n}}\right] = \ln A_\alpha = aE_\alpha + b \quad (10)$$

After that, the pre-exponential factor values are calculated by the CE formula using E_α.

The iterative equations of KAS (it-KAS) and FWO (it-FWO) used to calculate the activation energy are expressed as eqn (11) and (12):

$$\ln\frac{\beta_i}{h(x){T_{\alpha,i}}^2} = \ln\frac{A_\alpha R}{g(\alpha)} - \frac{E_\alpha}{RT_{\alpha,i}} \quad (11)$$

$$\ln\frac{\beta_i}{H(x)} = \ln\frac{0.0048A_\alpha E_\alpha}{g(\alpha)R} - 1.0516\frac{E_\alpha}{RT_{\alpha,i}} \quad (12)$$

i is the number of experiments, β_i to its corresponding heating rate and x, $h(x)$ and $H(x)$ formulas are, respectively, written as in eqn (13)–(15).

$$x = \frac{E_\alpha}{RT_{\alpha,i}} \quad (13)$$

$$h(x) = \frac{x^4 + 18x^3 + 86x^2 + 96x}{x^4 + 20x^3 + 120x^2 + 240x + 120} \quad (14)$$

$$H(x) = \frac{\exp(-x)h(x)/x^2}{0.0048\exp(-1.0516x)} \quad (15)$$

The conversion dependent pre-exponential factor A_α is obtained by using the calculated E_α values and the plots intercept of eqn (11) and (12).

Finally, the combination of the equation (eqn (16)) with the 41 forms of $g(\alpha)$ leads to define the reaction model.

$$\ln g(\alpha_i) = \left[\ln\frac{A_\alpha E_\alpha}{R} + \ln\frac{\exp(-x)}{x^2} + \ln h(x)\right] - \ln\beta_i \quad (16)$$

Vyazovkin methodology calculates for each conversion the E_α that minimizes the isoconversional nonlinear method of Vyazovkin (eqn (17)).

$$\varnothing(E_a) = \sum_i^n \sum_{j\neq i}^n \frac{I(E_\alpha, T_{\alpha,i})\beta_j}{I(E_\alpha, T_{\alpha,j})\beta_i} \quad (17)$$

where j and i stand for experiments performed under different heating β_i and n stand for the total number of experiments.

$$I(E_\alpha, T_\alpha) = \frac{E_\alpha}{R}f(x) \quad (18)$$

And

$$f(x) = \frac{E_\alpha}{R}\frac{x^4 + 18x^3 + 86x^2 + 96x}{x^4 + 20x^3 + 120x^2 + 240x + 120} \quad (19)$$

The pre-exponential factor is estimated by using the CE by a single heating rate method in the succeeding correlation eqn (20):

$$\ln A_i = aE_i + b \quad (20)$$

a, b: the compensation parameters.

After that, the reaction of model is mathematically determined using the values of E_α and A_α by using eqn (21).

$$g(\alpha) = \frac{A_\alpha}{\beta}\int_0^{T_\alpha}\exp\left(\frac{-E_\alpha}{RT}\right)\mathrm{d}T \quad (21)$$

It is worthy to mention that all revealed calculations were carried out by means of MATLAB software (a powerful tool for numerical calculation).

4. Results and discussion

4.1. Selecting the optimal HNTO/AN co-crystal

4.1.1. Based on the energy content. The thermal behavior of EMs is so important to understand since it plays an important role for the preparation, processing, and storage as well as for the evaluation of their utilization and performance.[49–52] DSC experiments were undertaken at 10 °C min^{-1} to investigate the thermal behavior of the prepared co-crystals. The obtained results are illustrated in Fig. 2A and summarized in Table 1. The trend of the DSC curves for the samples, which have molar ratios between 1 : 1 and 1 : 6 is almost similar for which only one peak decomposition temperature is appeared. It is worthy to mention that, according to DSC curves, co-crystals of HNTO/AN have been successfully prepared with molar ratios ranging from 1 : 1 to 1 : 6, whereas no co-crystals were obtained when using molar ratios of 1 : 7 and 1 : 9, which generated only physical mixtures. In fact, it is evident from the DSC curves that the thermal behavior of cocrystals is obviously different from that of the samples 1 : 7 and 1 : 9 (HNTO : AN). Besides, the cocrystals present only one strong exothermic peak, whereas, the two samples with molar ratios of 1 : 7 and 1 : 9 exhibits the behavior of the both pure components (HNTO and AN). SEM micrographs of the investigated samples confirm these results. As shown in Fig. 3A, a well-defined morphology (rod-like crystals) has been noticed for the co-crystal 1 : 3 (HNTO : AN), which is similar to the other co-crystals (molar ratio ranging from 1 : 1 to 1 : 6). However, in the case of samples with a molar ratios of 1 : 7 and 1 : 9, distinct pure HNTO and AN can be clearly observed, revealing that they correspond to physical mixtures.

However, such temperature is not constant and depends closely on the composition of the co-crystal, revealing that the nature of the interactions are different within the different samples.

On the other hand, a large difference, shown for the heat released during the decomposition process, can be observed. This latter is another important parameter to consider when characterizing EMs, since it dictates its performance.[35,36] As expected, the co-crystal (1 : 1) is presented with a considerably

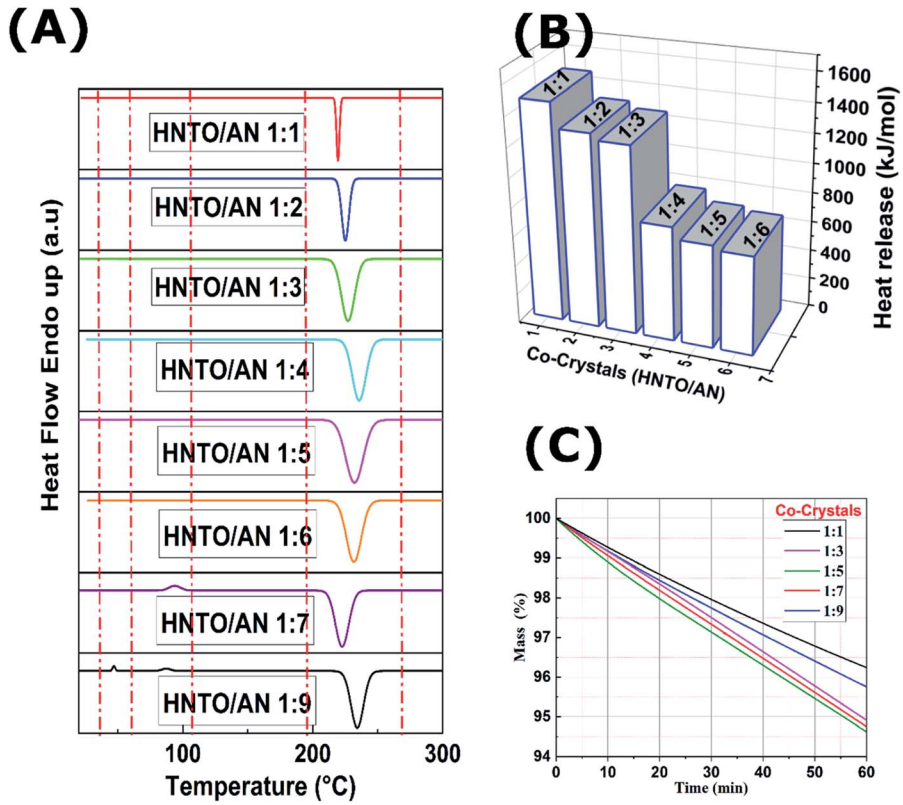

Fig. 2 (A) DSC curves of the obtained co-crystals with different molar ratios at heating rate of 10 °C min^{-1}, (B) heat release of the different obtained co-crystals with different molar ratios and (C) hygroscopicity of the obtained co-crystals with different molar ratios.

Table 1 Non-isothermal DSC data at heating rate of 10 °C min^{-1}

Molar ration	T_0 (°C)	T_P (°C)	T_e (°C)	ΔH (J g^{-1})
HNTO/AN (1 : 1)	215.2	226.9	229.3	1483.1
HNTO/AN (1 : 2)	230.9	232.4	235.3	1315.1
HNTO/AN (1 : 3)	235.1	239.3	241.5	1272.7
HNTO/AN (1 : 4)	230.3	241.0	250.2	780.1
HNTO/AN (1 : 5)	220.8	242.1	251.6	700.7
HNTO/AN (1 : 6)	226.9	232.5	246.8	673.6
HNTO/AN (1 : 7)	209.6	233.0	235.5	600.3
HNTO/AN (1 : 9)	230.2	239.6	257.8	537.3

high heat release value (1481 J g^{-1}), which is clearly shown in Fig. 1B, whereas (1 : 6) co-crystal exhibited the lowest value among all the samples (600 J g^{-1}). These results highlight that by rising the amount of AN within the co-crystal (HNTO/AN), the heat release decreases considerably. Besides, there is a huge decrease on heat released from co-crystal (1 : 4) (780 J g^{-1}) compared to those of (1 : 3) (1272.7 J g^{-1}) and (1 : 2) (1315.1 J g^{-1}). This allows deducing that the ratio of 1 : 3 ensures obtaining a co-crystal with a higher amount of AN that do not noticeably scarify the energy content, and hence acceptable performance is maintained.

4.1.2. Based on the hygroscopicity. The development of solid propellant oxidize less sensitive to the humidity is highly recommended, since it can ease its processing during the propellant formulation. Fig. 1C shows the isothermal TGA profiles of the different samples what display the elimination of the water content adsorbed on the sample surfaces. The determined moisture content for all samples is less than 6% for which the lowest value is obtained for the co-crystal 1 : 1 and the highest one corresponded to the sample of a molar ratio 1 : 6. This result may be attributed to the enhanced AN content on the obtained co-crystal, which is highly hygroscopic. Obviously, all the synthesized co-crystals have a reduced moisture content, which is an extremely significant and suitable for practical applications. Thus, in term of hygroscopicity, among the co-crystals with a higher amount of AN, that of 1 : 3 can be considered the best since it contained the lowest humidity content. On the other hand, a chaotic and random behavior was observed for compounds with a molar ratio of (1 : 7) and (1 : 9) because they are just a physical mixture.

4.1.3. Based on the density. The elaboration of high-energy dense materials becomes a hot research topic.[11,53] The increase of the density of energetic materials can directly improve their performance. The measured density values of the different co-crystals are gathered in Fig. 4A, and the results exhibited clearly that all the co-crystals presented a high density compared to pure AN (1.72). As expected, the highest density value is corresponded to the co-crystal (1 : 1) since it contained the highest amount of high-dense HNTO. It is worthy to note that the densities of the obtained compounds are within the same range as the most frequently utilized energetic materials such as like HMX and RDX.[54] On the other side, by drawing the

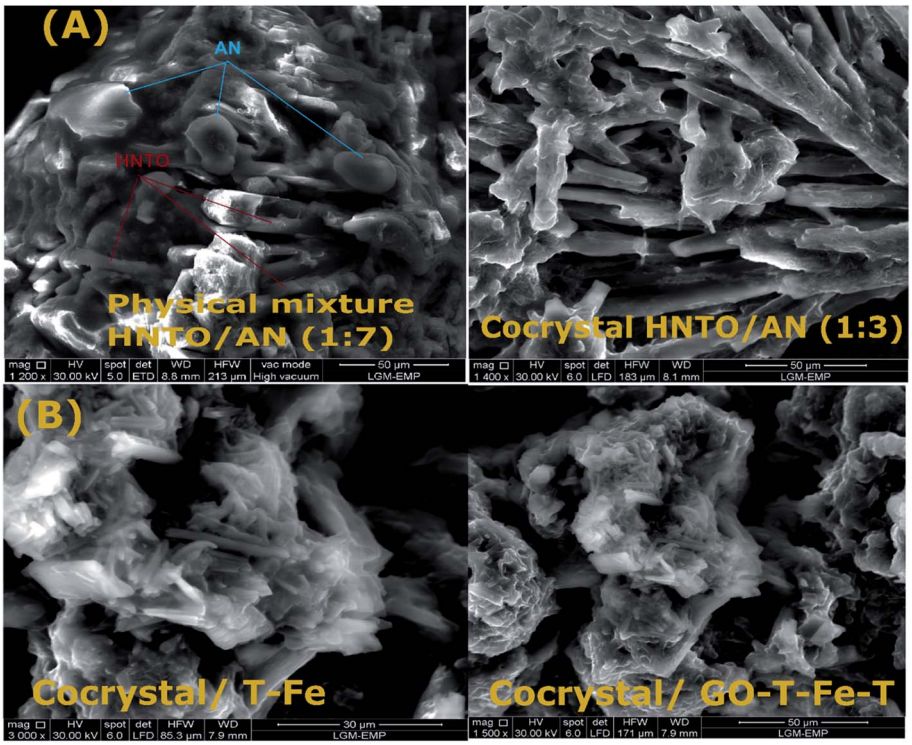

Fig. 3 SEM micrographs of (A) the different co-crystals prepared at different molar ratios, (B) the prepared composites: (HNTO/AN)/T-Co and (HNTO/AN)/GO-T-Co-T.

two tangents to the curve on either side, the intersection of the two tangents is at the appropriate density value corresponding to a high amount of AN, which obviously coincided with the ratio 1 : 3.

4.1.4. Based on the production cost. Reducing costs is commonly considered as one of key forces that drive the development of new compounds and materials.[55] Thus, taking in consideration the cost of the production of HNTO/AN co-crystals, at least in qualitative way, is so important. It is worthy to mention that HNTO is expensive than AN, since the raw-materials of the former are costly. Therefore, the decrease of the amount at a suitable ratio will certainly reduce the overall co-crystal production cost compared to the co-crystal having a ratio of 1 : 1. Based on the market prices of the raw materials as well as other additional costs such as production energy, experimental facilities, water, *etc.*, the obtained production costs of the different co-crystals are depicted in Fig. 4B. In light of these results, one may deduce that the co-crystal with

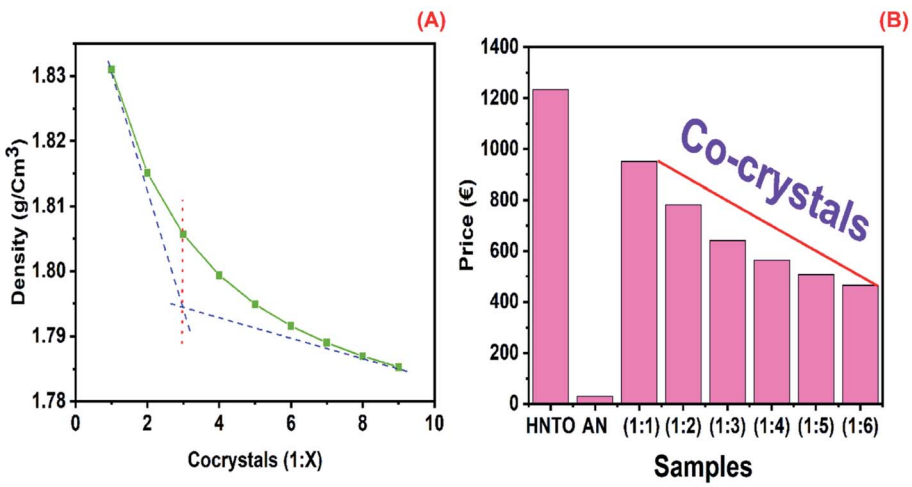

Fig. 4 (A) Density of the obtained co-crystals with different molar ratio, (B) estimated cost of one (1) kg of the co-crystals with different molar ratios.

a reduced amount of HNTO is the cheapest one. Accordingly, the best molar ratio, which may be chosen, corresponds to the co-crystal 1 : 3.

4.2. Comparison between the two co-crystals 1 : 1 and 1 : 3

4.2.1. Chemical structure. FTIR serves as suitable technique for the chemical analysis of molecular species. It is considered as an excellent method to study and characterize co-crystallization because the co-crystal formation is a result of interactions between different molecular components. The IR spectra of the two selected co-crystals are displayed in Fig. 5A. It is clear that the two samples gave exactly the same spectrum, proving that both samples present similar chemical structure, but with slight intensity differences caused probably by additional interactions between HNTO and AN raw compounds for which the spectra are displayed in ESI.† In fact, a group of frequencies situated within 3270–3354 cm^{-1} is allocated to the NH stretching vibration, whereas those at frequencies of 1648 to 1505 cm^{-1} are assigned to asymmetrical NO_2 stretching. A stretching vibration attributed to N–N band is also shown within 1000–1100 cm^{-1} region. The obtained result for the co-crystal 1 : 3 are in good accordance to those reported in our recent published article.[29]

4.2.2. Crystal structure. The XRD technique is one of indispensable method widely utilized for the material characterization. It can be employed to confirm the formation of co-crystals as well. The XRD of pure AN and HNTO are added as ESI.† Fig. 5B shows the XRD patterns of the as-developed co-crystals. The two samples gave exactly the same XRD structure, indicating once more the formation of the same compound. It is worth noting that the observed XRD patterns correspond well with those reported in the literature.[29] In fact, most of the characteristic diffraction peaks observed on the co-crystal 1 : 1 are present in the co-crystal 1 : 3. The main diffraction peaks of the two obtained co-crystals, corresponding to planes (011), (1−31), (311), (2−21), (11−1) and (1−11),

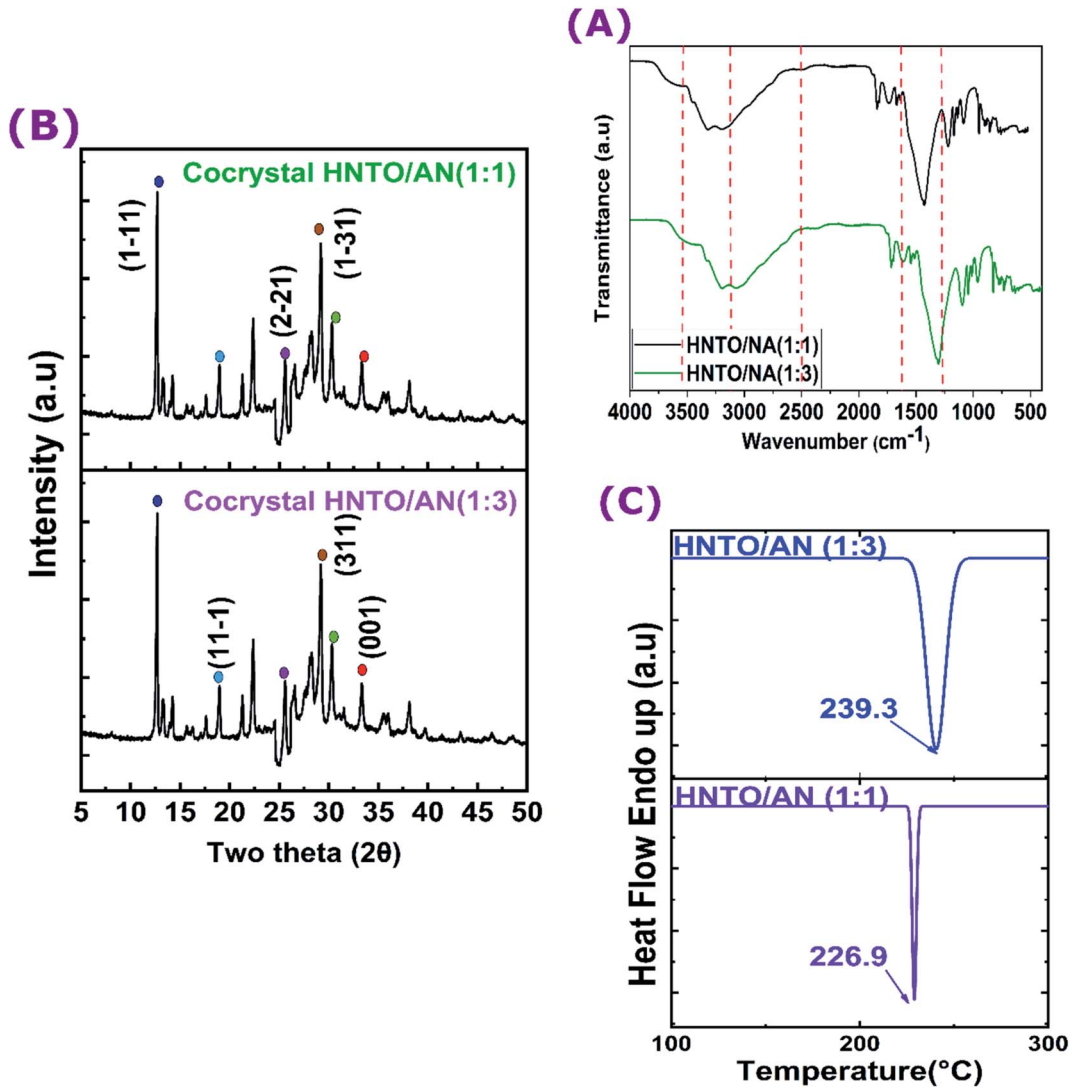

Fig. 5 (A) FTIR spectra of co-crystals with molar ratios of (1 : 1) and (1 : 3), (B) XRD of co-crystals HNTO/AN (1 : 1) and HNTO/AN (1 : 3) and (C) DSC curved of the two selected co-crystals.

provide a clear evidence for the development of the same product at a lower price and containing a higher amount of AN.

4.2.3. Thermal behavior. For the sake of comparing the heat change during the thermolysis of the two co-crystals, the DSC analyses have been carried out at a heating rate of 10 °C min^{-1}. The key findings in this section are summarized as follows: both of the two co-crystals have only one decomposition peak. As expected, the co-crystal with 1 : 3 molar ratio decomposes at a slightly higher with respect to that of the co-crystal 1 : 1, which may be probably due to the important amount of AN in the first co-crystal, causing a shift of its decomposition peak temperature to high value (Fig. 5C). Despite the heat released amount has decreased by enhancing the quantity of AN to 1273 J g^{-1}, while it was almost 1483 J g^{-1} in the case of the co-crystal 1 : 1, such new thermostable co-crystal contained a higher amount of AN compared to HNTO, considered as a promising oxidizer for composite solid propellants.[25] Moreover, the activation energy of the co-crystal 1 : 3 has been also calculated in order to compare it to that obtained for the co-crystal 1 : 1. It is worthy to mention that the activation energy is defined as the barrier of energy to overcome the initiation of the reaction of decomposition. Thus, when the value of activation energy (E_a) is high, the reaction rate is slow and the process is more difficult to occur. It can be clearly checked from Table 2 that higher value of E_a has been found for the co-crystal (1 : 3) compared to that of co-crystal (1 : 1), which is an indication of the improvement of the stability of the novel co-crystal.

4.3. Morphological structure of HNTO/AN@T-Co and HNTO/AN@GO-T-Co-T

The SEM is a powerful tool that provide valuable information about external crystal morphology. Based on SEM results depicted in Fig. 3B, both of GO-T-Co-T and T-Co energetic catalysts are well-dispersed on the surface of HNTO/AN. The agglomeration problem of nano-sized catalysts is avoided through the appropriate mixing with the cocrystal, as demonstrated in our previous study for other composites.[36] Moreover, the presence of GO as the supported dispersion media, which allows a better dispersion of Co, improved the decomposition process of the cocrystal that may improve the final performance of the derived energetic formulations such as solid propellants.

4.4. Effect of energetic catalysts on the thermal decomposition of the co-crystal 1 : 3

To well highlight the thermal behavior of the co-crystal 1 : 3 mixed with the two energetic catalysts, the decomposition temperature as well as the heat release during the decomposition were determined and the results are reported in Table 3. The non-isothermal DSC curves of the pure co-crystal, the co-crystal/T-Co complex and the co-crystal/GO-T-Co-T complex are illustrated in Fig. 6. It is clearly found that all the studied samples exhibited one decomposition peak temperature. The pristine co-crystal decomposes at around 239.3 °C with a sharp

Table 3 Heat flow and decomposition temperature at heating rate of 10 °C min^{-1}

Compounds	Tp	Heat release J g^{-1}
Cocrystal (1 : 3)	239.3	1272.7
Cocrystal/T-Co	185.7	1302.0
Cocrystal/GO-T-Co-T	149.4	3262.0

Table 2 Kinetic triplet of the developed cocrystal HNTO/AN (1 : 3) with and without catalysts utilizing four isoconversional method

			Kinetic parameters		
Samples	Isoconversional method		$E_{a_{av}}$ (kJ mol^{-1})	Log(A) (s^{-1})	Integral reaction mechanism ($g(\alpha)$)
HNTO-AN (1 : 3)	TAS		179 ± 7	16.7 ± 0.7	13 $P_{1/4}$
	it-KAS		179 ± 7	16.7 ± 0.7	12 $P_{1/3}$
	it-FWO		174 ± 7	16.6 ± 0.7	12 $P_{1/3}$
	VYA	$\beta = 5$ °C min^{-1}	179 ± 7	17.1 ± 0.7	—
		$\beta = 10$ °C min^{-1}		17.4 ± 0.7	—
		$\beta = 15$ °C min^{-1}		17.6 ± 0.7	—
		$\beta = 20$ °C min^{-1}		17.7 ± 0.7	—
HNTO/AN (1 : 3)/T-Co	TAS		86 ± 11	7 ± 1	22 A_2
	it-KAS		86 ± 11	5 ± 1	37 D_6
	it-FWO		85 ± 11	5 ± 1	37 D_6
	VYA	$\beta = 5$ °C min^{-1}	86 ± 11	6 ± 1	—
		$\beta = 10$ °C min^{-1}		7 ± 1	—
		$\beta = 15$ °C min^{-1}		7 ± 1	—
		$\beta = 20$ °C min^{-1}		7 ± 1	—
HNTO/AN (1 : 3)/GO-T-Co-T	TAS		98 ± 7	10 ± 1	24 A_4
	it-KAS		98 ± 7	8 ± 2	35 D_4
	it-FWO		96 ± 7	8 ± 2	35 D_4
	VYA	$\beta = 5$ °C min^{-1}	98 ± 7	10 ± 1	—
		$\beta = 10$ °C min^{-1}		10 ± 1	—
		$\beta = 15$ °C min^{-1}		10 ± 1	—
		$\beta = 20$ °C min^{-1}		11 ± 1	—

exothermic peak. When T-Co catalyst is added, the decomposition peak temperature (Tp) was decreased by around 55 °C. This finding indicates that the catalyst T-Co has a significant catalytic effect on the thermolysis of the developed co-crystal. After the incorporation of GO-T-Co-T, the Tp of the co-crystal has dramatically decreased from 239.3 °C to 149.4 °C, which indicates that the GO-T-Co-T catalyst has a similar excellent catalytic efficiency than T-Co on the decomposition of the co-crystal. Nevertheless, the heat release obtained for the pure co-crystal is about 1273 J g^{-1}, which is close to that containing T-Co as catalyst and much lower than that supplemented with GO-T-Co-T (3262.6 J g^{-1}). This results maybe attributed to improvement of thermal conductivity of the HNTO/AN co-crystal owing to the presence of GO, which improves the catalytic effect of the complex on the solid/liquid/gas phase as well. In light of these obtained results, one may confirm once more the prominent performance of the developed co-crystal/catalyst system, since a strong decomposition heat release has been noticed.

4.5. Determination of kinetic parameters

The main goal of thermal decomposition experiments is to acquire accurate information on the reaction mechanism and the Arrhenius parameters of the degradation of EMs.[36] It is well known that the apparent energy of activation calculated by isoconversional method displays more detailed information about the process of thermal decomposition.[48,56] The thermal decomposition kinetics of the pure co-crystal HNTO/AN and its composites with T-Co and GO-T-Co-T are studied by using kinetic isoconversional approaches, namely, it-FWO, it-KAS, VYA and TAS. E_a, log(A) and the most probable mathematical reaction model are estimated based on DSC data. The typical DSC thermograms for the three samples at different heating rates are presented in Fig. 7A. It is well shown that all the studied systems exhibit only one exothermic peak. Furthermore, it is clear that, the decomposition temperatures shifted to higher values by increasing the heating rate.

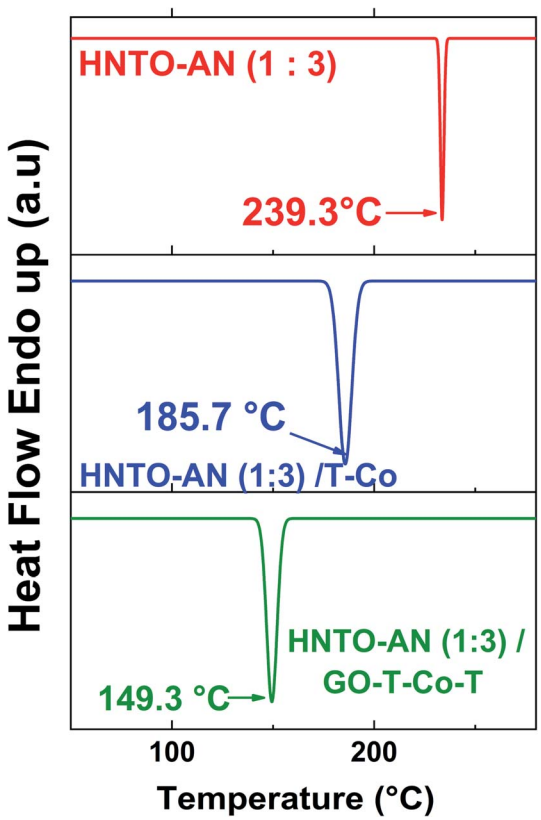

Fig. 6 DSC curves of the two selected co-crystals at 10 °C min^{-1}.

The average values of the kinetics parameters and the reaction model achieved by the four employed isoconversional methods are described in Table 2. Furthermore, the resultant averaged relative errors for both apparent activation energy and log(A) are, respectively, 16.61% and 19.99% for the developed co-crystal, 11.64% and 14.17% for co-crystal/T-Co, 24.41% and 29.95% for co-crystal/GO-T-Co-T. An excellent accuracy has been shown for the obtained E_a calculated by the different isoconversional linear approaches since the linear correlation coefficients (R^2) are within the range of 0.9980–0.9998.

As shown in Fig. 7B, the obtained Arrhenius parameters for the different samples have the same trend. Similarly, it may be noticeably checked that, except the Arrhenius parameters estimated based on it-FWO, others present close values. This may be due to the fact that this method utilizes only the first approximation of the temperature integral, as it is well illustrated in Fig. 7B, C and Table 2.

In fact, the average value of E_a of the co-crystal is around 179, whereas those of the co-crystal/T-Co and the co-crystal/GO-T-Co-T, are not available in literature, have been reduced, confirming the catalytic effect of the energetic complexes as shown in Fig. 7 and Table 2. T-Co has greatly decreased the value of the energy of activation from 179 to 86 kJ mol^{-1}, proving once more the stronger catalytic effect of this kind of catalysts on the decomposition of HNTO/AN co-crystal. Similar behavior has been remarked for the effect of this kind of catalyst on decomposition of NTO.[36] On the other hand, the use of GO-T-Co-T led to the decrease of the activation energy of the co-crystal by about 80 kJ mol^{-1}, owing to the important heat-transfer ensured by the GO, which may promote the heat transfer through the thermolysis of the obtained co-crystal and accelerating the chemical reaction. Besides that, the nanoscale structure of the used GO can lead to the formation of lots of localized hotspots that can stimulate the thermal decomposition at lower temperature and lower activation energy. Besides that, it can be inferred from Fig. 7 that the evolution of E_a in function of the extent of conversion of the pure co-crystal is different from those containing catalysts. For the pure co-crystal, it increases first and then decreases feebly when the extent of conversion exceed 0.2, whereas that of the composite co-crystal/GO-T-Co-T increased slightly until the end of conversion. In the case of the composite co-crystal/T-Co, the obtained trend of E_a decreases at first and then increases after a certain value of conversion ($\alpha > 0.4$).

On the other hand, based on the reaction models given in our previous work,[43] the reaction models of the studied composites are estimated to check the inherent mechanisms

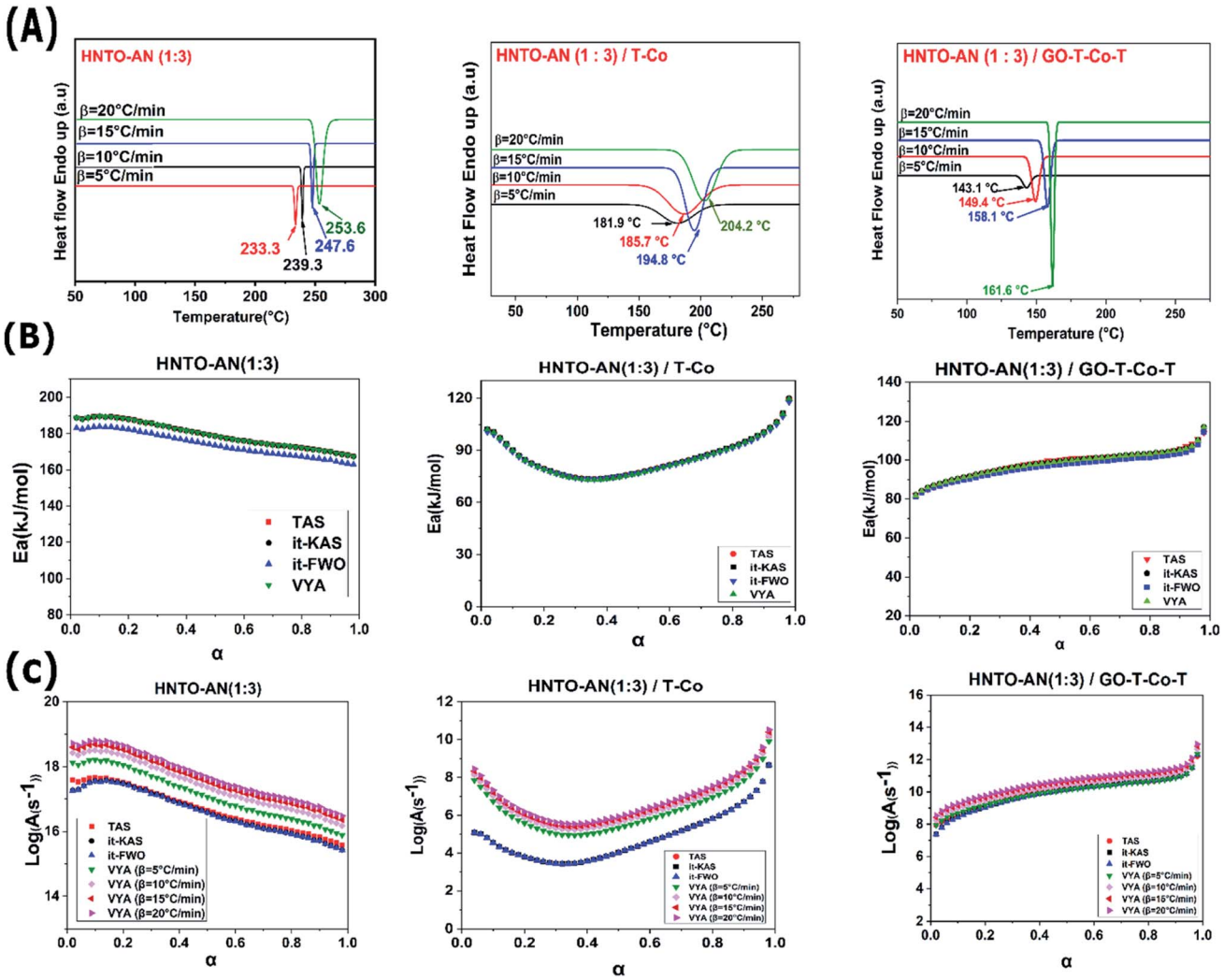

Fig. 7 (A) Non-isothermal DSC of pure co-crystal (1 : 3), (HNTO/AN)/T-Co and (HNTO/AN)/GO-T-Co-T at different heating rates, (B) evolution of the activation energy in function of conversion for HNTO/AN (1 : 3) with and without catalysts; (C) log(*A*) for HNTO/AN with and without catalysts.

related to the influence of the used catalysts on the co-crystal decomposition. As seen in Fig. 8A and Table 2, the investigated systems follow diverse reaction mechanisms during their decomposition. It turns out that each sample follows different probable theoretical integral model by using TAS method, whereas, it-KAS and it-FWO in the three cases provide the same mechanism for each sample. On the other hand, only numerical values of the experimental integral model are furnished by using VYA approach.[47,57] Concerning it-FWO and it-KAS methods, the thermal decomposition of the co-crystal, the co-crystal/T-Co and the co-crystal/GO-T-Co-T follows the Avrami–Erofeev mechanism (random nucleation model), three-dimensional diffusion mechanism (Ginstling–Brounshtein) and 3D diffusion mechanism, respectively. These differences may be principally affected by the nature of the samples and the different approximations utilized by each isoconversional technique.[43] Moreover, under the effect of T-Co, the decomposition moves more or less to the two-dimensional growth of the nuclei model (A_2), indicating that the decomposition initiates at the surface of catalysts where cobalt ions is considered as the active points.

The evolution of the activation energy and *A* along with their associated uncertainty intervals computed using TAS methodology with extent of conversion for the thermal decomposition of the investigated samples are reported in Fig. 8B as well. From the obtained results, one may deduce that the relative errors of E_a and log(*A*) are very close which confirm their comparable accuracy.[40,43]

5. Conclusions

HNTO/AN co-crystal with an optimized molar ratio has been successfully synthesized. Several criteria were used to select the best molar ration such as the heat release, density, cost and water content. The results showed that the co-crystal with the molar ratio of 1 : 3 (HNTO/AN) displayed interesting

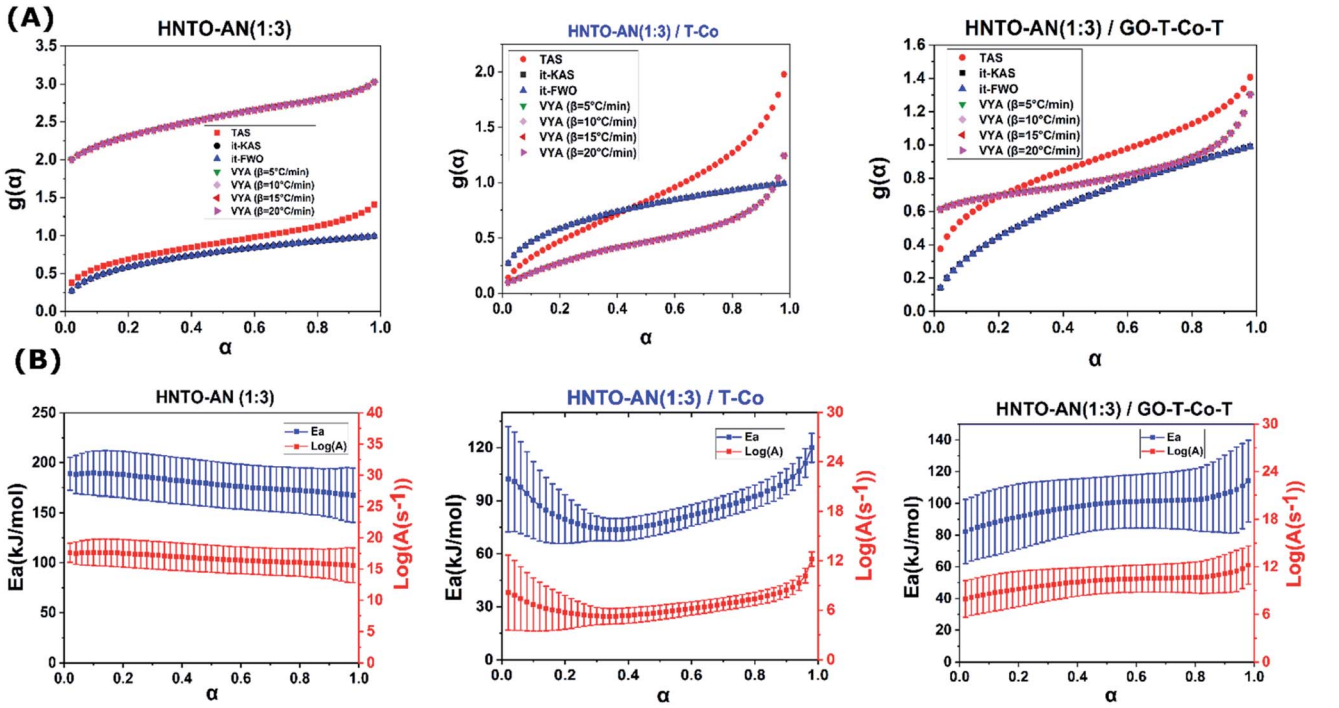

Fig. 8 (A) Evolution of the integral reaction model values in function of conversion for the different samples, (B) E_a and log(A) and their associated errors progress as a function of conversion for the cocrystal with and without catalysts.

characteristics such as good thermal stability, high density and energy content and lower production cost, even with the co-crystal with a molar ratio of 1 : 1. The effect of two energetic coordination polymers on the thermal decomposition behavior of the co-crystal as well as its decomposition kinetics were, respectively, carried out by utilizing DSC and the isoconverional kinetic methods. The employed cobalt-based materials (T-Co and GO-T-Co-T) have revealed a noticeable catalysis effect on the thermal decomposition process of the HNTO/AN co-crystal, especially in reducing the mean value of the activation energy and decomposition temperature. Finally, the developed product, with outstanding energy content and good thermal stability, can be considered as a prominent oxidizing system, which can find suitable applications in solid propellant and explosive formulations.

Conflicts of interest

There are no conflicts to declare.

References

1 A. Benhammada and D. Trache, *Appl. Spectrosc. Rev.*, 2020, **55**, 724–777.
2 D. Trache and L. T. DeLuca, *Nanomaterials*, 2020, **10**, 2347.
3 W. Pang, L. T. DeLuca, A. A. Gromov and A. S. Cumming, *Innovative Energetic Materials: Properties, Combustion Performance and Application*, Springer, 2020.
4 T. M. Klapötke, *Energetic Materials Encyclopedia*, De Gruyter, 2018.
5 M. H. Keshavarz and T. M. Klapötke, *The properties of energetic materials*, De Gruyter, 2017.
6 V. E. Zarko and A. A. Gromov, *Energetic nanomaterials: synthesis, characterization, and application*, Elsevier, 2016.
7 L. Feng, D. Cao, J. Wang, P. Liu and N. Zhang, *Chin. J. Energ. Mater.*, 2015, **23**, 376–385.
8 B. Tan, M. Huang, X. Long, J. Li, X. Yuan and R. Xu, *Int. J. Quantum Chem.*, 2015, **115**, 84–89.
9 R. P. Singh, R. D. Verma, D. T. Meshri and J. n. M. Shreeve, *Angew. Chem., Int. Ed.*, 2006, **45**, 3584–3601.
10 H. Gao and J. n. M. Shreeve, *Chem. Rev.*, 2011, **111**, 7377–7436.
11 Q.-L. Yan, F.-Q. Zhao, K. K. Kuo, X.-H. Zhang, S. Zeman and L. T. DeLuca, *Prog. Energy Combust. Sci.*, 2016, **57**, 75–136.
12 M. S. Gruhne, M. Lommel, M. H. Wurzenberger, T. M. Klapötke and J. r. Stierstorfer, *Inorg. Chem.*, 2021, **60**, 4816–4828.
13 N. V. Muravyev, D. B. Meerov, K. A. Monogarov, I. N. Melnikov, E. K. Kosareva, L. L. Fershtat, A. B. Sheremetev, I. L. Dalinger, I. V. Fomenkov and A. N. Pivkina, *Chem. Eng. J.*, 2021, **421**, 129804.
14 Z.-H. Xue, X.-X. Zhang, B. Huang, J. Cheng, K. Wang, Z. Yang and Q.-L. Yan, *Crystal Growth & Design*, 2021.
15 X.-X. Zhang, Z.-J. Yang, F. Nie and Q.-L. Yan, *Energetic Materials Frontiers*, 2020.
16 M. K. Bellas and A. J. Matzger, *Angew. Chem., Int. Ed.*, 2019, **58**, 17185–17188.
17 J. Yang, L. Yin, X.-D. Gong, V. P. Sinditskii and J.-G. Zhang, *Cryst. Growth Des.*, 2020, **20**, 5834–5842.

18 Y. Liu, C. An, J. Luo and J. Wang, *Acta Crystallogr., Sect. B: Struct. Sci., Cryst. Eng. Mater.*, 2018, **74**, 385–393.
19 L. Bao, P. Lv, T. Fei, Y. Liu, C. Sun and S. Pang, *J. Mol. Struct.*, 2020, 128267.
20 J. C. Bennion and A. J. Matzger, *Acc. Chem. Res.*, 2021, **54**, 1699–1710.
21 J. Zhang, J. P. Hooper, J. Zhang and M. S. Jean'ne, *Chem. Eng. J.*, 2021, **405**, 126623.
22 Y. Tan, Y. Liu, H. Wang, H. Li, F. Nie and Z. Yang, *Cryst. Growth Des.*, 2020, **20**, 3826–3833.
23 C. Oommen and S. Jain, *J. Hazard. Mater.*, 1999, **67**, 253–281.
24 J. Jos and S. Mathew, *Crit. Rev. Solid State Mater. Sci.*, 2017, **42**, 470–498.
25 D. Trache, T. M. Klapötke, L. Maiz, M. Abd-Elghany and L. T. DeLuca, *Green Chem.*, 2017, **19**, 4711–4736.
26 T. Lee, J. W. Chen, H. L. Lee, T. Y. Lin, Y. C. Tsai, S.-L. Cheng, S.-W. Lee, J.-C. Hu and L.-T. Chen, *Chem. Eng. J.*, 2013, **225**, 809–817.
27 P. Kumar, P. C. Joshi and R. Kumar, *Combust. Flame*, 2016, **166**, 316–332.
28 I. Oluwoye, M. Altarawneh, J. Gore and B. Z. Dlugogorski, *Combust. Flame*, 2020, **213**, 132–139.
29 S. Hanafi, D. Trache, R. Meziani, H. Boukciat, A. Mezroua, A. F. Tarchoun and M. Derradji, *Chem. Eng. J.*, 2021, 128010.
30 A. Benhammada and D. Trache, *J. Therm. Anal. Calorim.*, 2021, 1–16.
31 A. Benhammada, D. Trache, S. Chelouche and A. Mezroua, *Z. Anorg. Allg. Chem.*, 2021, **647**, 312–325.
32 A. Benhammada, D. Trache, M. Kesraoui and S. Chelouche, *Nanomaterials*, 2020, **10**, 968.
33 H. Kechit, S. Belkhiri, A. K. Bhakta, D. Trache, Z. Mekhalif and A. F. Tarchoun, *Z. Anorg. Allg. Chem.*, 2021, **647**(16–17), 1607–1619.
34 Q.-L. Yan, M. Gozin, F.-Q. Zhao, A. Cohen and S.-P. Pang, *Nanoscale*, 2016, **8**, 4799–4851.
35 S. Hanafi, D. Trache, W. He, W.-X. Xie, A. Mezroua and Q.-L. Yan, *J. Phys. Chem. C*, 2020, **124**, 5182–5195.
36 S. Hanafi, D. Trache, W. He, W.-X. Xie, A. Mezroua and Q.-L. Yan, *Thermochim. Acta*, 2020, **692**, 178747.
37 Z. Wu, J. Pei, X. Song, N. Liu, J. Li, M. Zhang, J. Zhang, D. Zhang and F. Zhao, *New J. Chem.*, 2020, **44**, 1858–1864.
38 J.-H. Yi, F.-Q. Zhao, Y.-H. Ren, S.-Y. Xu, H.-X. Ma and R.-Z. Hu, *J. Therm. Anal. Calorim.*, 2010, **100**, 623–627.
39 M. Zhang, C. Li, H. Gao, W. Fu, Y. Li, L. Tang and Z. Zhou, *J. Mater. Sci.*, 2016, **51**, 10849–10862.
40 A. F. Tarchoun, D. Trache, T. M. Klapötke, S. Chelouche, M. Derradji, W. Bessa and A. Mezroua, *Macromol. Chem. Phys.*, 2019, **220**, 1900358.
41 H. Xu, X. Duan, H. Li and C. Pei, *RSC Adv.*, 2015, **5**, 95764–95770.
42 S. Vyazovkin, in *Isoconversional kinetics of thermally stimulated processes*, Springer, 2015, pp. 1–25.
43 D. Trache, A. Abdelaziz and B. Siouani, *J. Therm. Anal. Calorim.*, 2017, **128**, 335–348.
44 L. Liqing and C. Donghua, *J. Therm. Anal. Calorim.*, 2004, **78**, 283–293.
45 S. Vyazovkin, *Isoconversional kinetics of thermally stimulated processes*, Springer, 2015.
46 S. Genieva, L. Vlaev and A. Atanassov, *J. Therm. Anal. Calorim.*, 2010, **99**, 551–561.
47 S. Chelouche, D. Trache, A. F. Tarchoun, A. Abdelaziz, K. Khimeche and A. Mezroua, *Thermochim. Acta*, 2019, **673**, 78–91.
48 S. Vyazovkin, A. K. Burnham, J. M. Criado, L. A. Pérez-Maqueda, C. Popescu and N. Sbirrazzuoli, *Thermochim. Acta*, 2011, **520**, 1–19.
49 D. Guo and Q. An, *ACS Appl. Mater. Interfaces*, 2018, **11**, 1512–1519.
50 Q. L. Yan and S. Zeman, *Int. J. Quantum Chem.*, 2013, **113**, 1049–1061.
51 A. Mezroua, K. Khimeche, M. H. Lefebvre, M. Benziane and D. Trache, *J. Therm. Anal. Calorim.*, 2014, **116**, 279–286.
52 A. F. Tarchoun, D. Trache, T. M. Klapötke, M. Belmerabet, A. Abdelaziz, M. Derradji and R. Belgacemi, *Ind. Eng. Chem. Res.*, 2020, **59**, 22677–22689.
53 Q. Wang, Y. Shao and M. Lu, *Cryst. Growth Des.*, 2018, **18**, 6150–6154.
54 V. V. Zhurov, E. A. Zhurova, A. I. Stash and A. A. Pinkerton, *Acta Crystallogr., Sect. A: Found. Crystallogr.*, 2011, **67**, 160–173.
55 D. Badgujar, M. Talawar, S. Asthana and P. Mahulikar, *J. Hazard. Mater.*, 2008, **151**, 289–305.
56 S. Chelouche, D. Trache, A. F. Tarchoun, A. Abdelaziz and K. Khimeche, *J. Energ. Mater.*, 2020, **38**, 48–67.
57 S. Vyazovkin, A. K. Burnham, L. Favergeon, N. Koga, E. Moukhina, L. A. Pérez-Maqueda and N. Sbirrazzuoli, *Thermochim. Acta*, 2020, 178597.